Mon. Not. R. Astron. Soc. **395,** 1015–1020 (2009) doi:10.1111/j.1365-2966.2009.14596.x

Recent torque reversal of 4U 1907+09

S. Ç. İnam,[1⋆] Ş. Şahiner[2⋆] and A. Baykal[2⋆]

[1]*Department of Electrical and Electronics Engineering, Başkent University, 06530 Ankara, Turkey*
[2]*Physics Department, Middle East Technical University, 06531 Ankara, Turkey*

Accepted 2009 February 3. Received 2009 February 3; in original form 2008 December 22

ABSTRACT

We present timing and spectral analysis of *RXTE*-PCA (Proportional Counter Array) observations of the accretion powered pulsar 4U 1907+09 between 2007 June and 2008 August. 4U 1907+09 had been in a spin-down episode with a spin-down rate of -3.54×10^{-14} Hz s^{-1} before 1999. From *RXTE* observations after 2001 March, the source showed a ∼60 per cent decrease in spin-down magnitude, and *INTEGRAL* observations after 2003 March showed that source started to spin-up. We found that the source recently entered into a new spin-down episode with a spin-down rate of -3.59×10^{-14} Hz s^{-1}. This spin-down rate is pretty close to the previous long-term spin-down rate of the source measured before 1999. From the spectral analysis, we showed that hydrogen column density varies with the orbital phase.

Key words: accretion, accretion discs – stars: neutron – pulsars: individual: 4U 1907+09 – X-rays: binaries.

1 INTRODUCTION

4U 1907+09 is a high-mass X-ray binary (HMXB) system discovered by the Uhuru survey (Giacconi et al. 1971). The system consists of an X-ray pulsar accreting mass from a blue supergiant companion star. An orbital period of 8.38 d was found from Ariel V observations (Marshall & Ricketts 1980). Makishima et al. (1984) found the spin period value of 437.5 s using Tenma observations. Eccentricity of the orbit of the system was found to be ∼0.16 from *EXOSAT* observations (Cook & Page 1987). From *RXTE* observations, in't Zand, Baykal & Strohmayer (1998) found revised orbital parameters of the system. The evidence of two phase-locked flares at the folded orbital profile was reported (Marshall & Ricketts 1980; in't Zand et al. 1998). The presence of the two flares per orbit leaded to the suggestion of an equatorial-disc-like envelope around a Be-type stellar companion (Cook & Page 1987). Although the variation in Hα emission in the optical observations strengthened the suggestion of a Be star (Iye 1986), Cox, Kaper & Mokiem (2005) suggested the possibility of an OB supergiant companion previously mentioned by Schwartz et al. (1980) and van Kerkwijk, van Oijen & van den Heuvel (1989). Cox et al. (2005) identified the companion as an O8–09 Ia supergiant with a distance of ∼5 kpc.

4U 1907+09 had been steadily spinning down for more than 15 yr with an average rate of $\dot{\nu} = -3.54 \times 10^{-14}$ Hz s^{-1} (Cook & Page 1987; in't Zand et al. 1998; Baykal et al. 2001; Mukerjee et al. 2001). Afterwards, *RXTE* observations in 2001 showed ∼60 per cent decrease in the magnitude of the spin-down rate (Baykal, İnam & Beklen 2006). It has recently been reported that the pulse period evolution has shown a torque reversal with 2.58×10^{-14} Hz s^{-1}, confirming a spin-up episode after 2003 March (Fritz et al. 2006).

Spectral studies (Marshall & Ricketts 1980; Schwartz et al. 1980; Makishima et al. 1984; Cook & Page 1987; Chitnis et al. 1993; in't Zand, Strohmayer & Baykal 1997; Coburn et al. 2002) on 4U 1907+09 indicate a highly variable hydrogen column density over the binary orbit, between $\sim 1 \times 10^{22}$ and $\sim 9 \times 10^{22}$ cm^{-2}. The power-law photon index is between ∼0.8 and ∼1.5 with a high-energy cut-off around ∼13 keV. Extensive energy spectra generated from *Ginga* (Mihara 1995; Makishima et al. 1999) and *BeppoSAX* (Cusumano et al. 1998) observations exhibit absorption features at ∼19 and ∼39 keV referring to the fundamental and the second harmonic of a cyclotron absorption feature corresponding to a surface magnetic field strength 2.1×10^{12} G.

In this paper, we present timing and spectral analysis of *RXTE* monitoring observations of 4U 1907+09 between MJD 54280 and MJD 54690. First, we provide a brief description of observation and analysis procedure in Section 2. The pulse timing analysis, indicating a new spin-down episode, is reported in Section 3. In Section 4, we present the results of X-ray spectral analysis.

2 OBSERVATIONS AND DATA ANALYSIS

The analysis of *RXTE* monitoring observations of 4U 1907+09 is presented in this paper. The observations between 2007 June and 2008 August are analysed, each having an average exposure time ∼2 ks (see Fig. 1). The data products of Proportional Counter Array (PCA) on-board *RXTE* have been reduced for the analysis. *RXTE*-PCA is a pointed instrument (Jahoda et al. 1996); it consists of five co-aligned identical proportional counter units (PCUs) sensitive in the energy range 2–60 keV. The effective area of each detector is

⋆E-mail: inam@baskent.edu.tr (SÇİ); seyda@astroa.physics.metu.edu.tr (ŞŞ); altan@astroa.physics.metu.edu.tr (AB)

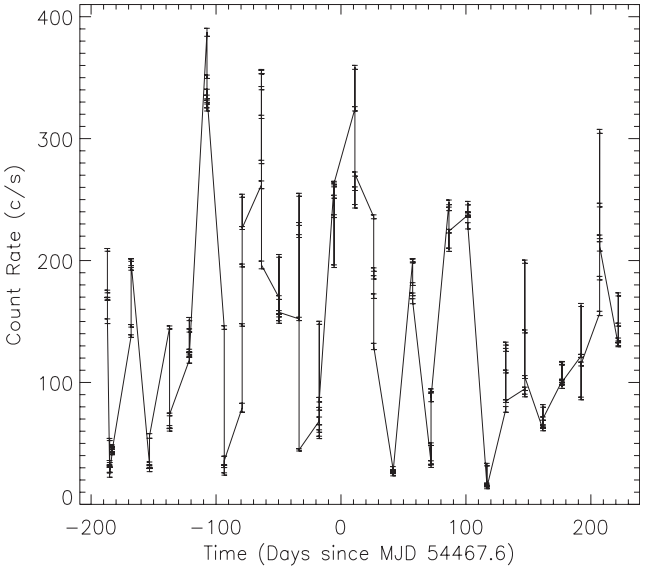

Figure 1. 440-s binned light curve of 4U 1907+09.

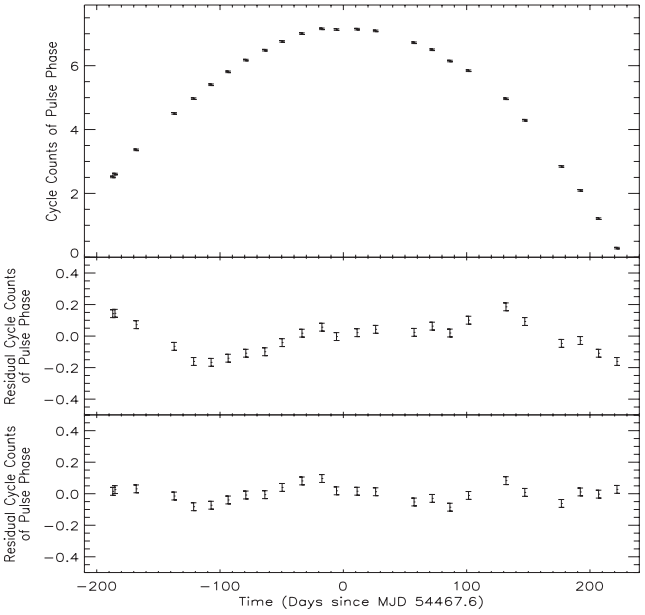

Figure 2. Pulse phase and its residuals after the removal of quadratic (middle panel) and cubic (lower panel) polynomials.

approximately ∼1300 cm^2, and the energy resolution is 18 per cent at 6 keV. A field of view (FOV) of 1° at full width at half-maximum (FWHM) is small enough that, with the large geometric area, PCA provides a highly sensitive time resolution. Operations are carried on with various PCUs turned off during observations in order to extend the lifetime of the instrument. The number of running PCUs during the observations of 4U 1907+09 varies between one and three. PCU0 and PCU1 have increased background levels due to the loss of their propane layers. As it is not recommended to use data of these PCUs for spectral analysis, data of PCU2 were used during spectral analysis. No PCU selection is done for the timing analysis, since propane losses do not affect high-resolution timing.

The standard *RXTE* analysis software HEASOFT 6.4 is used for data reduction. The Standard2f mode data with 128 energy channels are examined for the spectral analysis. Since the timing resolution of Standard2f is low, the GoodXenon mode data are used for the timing analysis using 1-s long binning. The filtering applied to the data is comprised excluding the times when, elevation angle is less than 10° and offset from the source is greater than 0.02. Electron contamination of PCU2 is also confirmed to be less than 0.1. The latest PCA background estimator models supplied by the *RXTE* Guest Observer Facility (GOF), Epoch 5C are used to generate the background light curves and spectra. The model estimation is based on the rate of very large solar events, spacecraft activation and cosmic X-ray emission. Since 4U 1907+09 is near the Galactic plane and the supernova remnant W49B, additional background estimation is done for X-ray spectral analysis (see Section 4).

3 TIMING ANALYSIS

For timing analysis, the background subtracted light curves were corrected to the barycentre of the Solar system and to the binary orbital motion of 4U 1907+09. For the correction of binary orbital motion, we used the orbital parameters deduced by in't Zand et al. (1998). We folded the ∼2-ks long light-curve segments outside intensity dips on statistically independent trial periods (Leahy et al. 1983). A template pulse profile was obtained from the first three observations with a total exposure of ∼6 ks by folding the data on the period giving the maximum χ^2. These three observations were made within the first week after the observations started. Template pulse profile was analytically represented by its Fourier harmonics (Deeter & Boynton 1985) and cross-correlated with the harmonic representation of average pulse profiles from each ∼2-ks long observation. The pulse phases calculated from this analysis are presented in Fig. 2.

To estimate pulse frequency derivatives, the pulse phases were fitted to the polynomial:

$$\delta\phi = \phi_o + \delta\nu(t - t_o) + \frac{1}{2}\dot{\nu}(t - t_o)^2 + \frac{1}{6}\ddot{\nu}(t - t_o)^3, \quad (1)$$

where $\delta\phi$ is the pulse phase offset deduced from the pulse timing analysis, t_o is the mid-time of the observation, ϕ_o is the phase offset at t_o, $\delta\nu$ is the deviation from the mean pulse frequency (or additive correction to the pulse frequency), $\dot{\nu}$ and $\ddot{\nu}$ are the first and second pulse frequency derivatives of the source. The pulse phases and the residuals of the fit after the removal of the quadratic (without the cubic term in equation 1) and cubic polynomial (equation 1) are also presented in Fig. 2. Timing solution of the source is presented in Table 1.

The pulse frequency derivative from the sequence of 25 pulse phases from the observations between 2007 June and 2008 August was measured as $-3.59(2) \times 10^{-14}$ Hz s^{-1}. This measurement shows that the source started to spin-down with a spin-down rate close to long-term spin-down rate of the source (Baykal et al. 2001).

Table 1. Timing solution of 4U 1907+09.

Parameter	Value
Epoch	MJD 54467.6(1) d
Orbital period	8.3753(1)
Projected semimajor axis (lt s)	83(2)
Eccentricity	0.28(4)
Longitude of periastron	330(7)
Spin frequency (ν)	$2.266460(2) \times 10^{-3}$ Hz
Spin frequency derivative ($\dot{\nu}$)	$-3.59(2) \times 10^{-14}$ Hz s^{-1}
$\ddot{\nu}$	$-5.3(4) \times 10^{-22}$ Hz s^{-2}

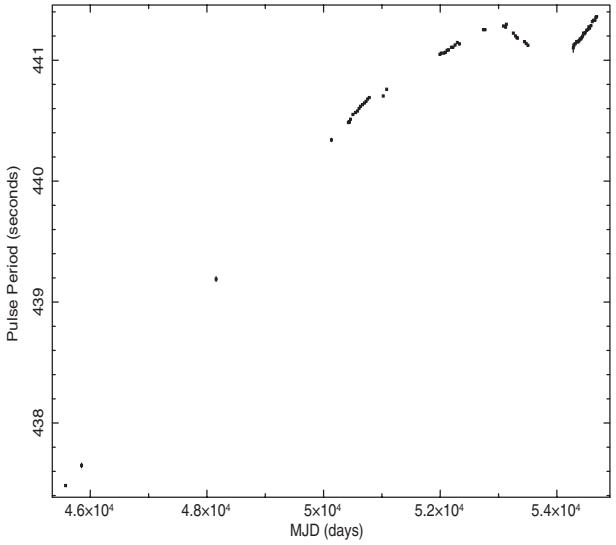

Figure 3. Pulse period measurements of 4U 1907+09. Recent spin-down trend of the source is evident between MJD 54281 and MJD 54682.

To demonstrate the torque reversal and show the recent spin-down trend of the source, we estimated the pulse frequency histories by taking the derivatives of each pairs of pulse phases from the pulse phases of this work. We presented pulse frequency history of the source in Fig. 3, and listed all pulse period measurements in Table 2.

4 SPECTRAL ANALYSIS

The energy range of the spectral analysis was restricted to 3–25 keV range since PCA count statistics is poor beyond 25 keV. Along with the basic estimation of PCA background models, additional background model was needed because 4U 1907+09 is near the Galactic plane and the supernova remnant W49B. During the dip states of 4U 1907+09, no pulsed emission was observed and the count rate was consistent with the diffuse emission from the Galactic ridge (in't Zand et al. 1997). About 20 per cent of the processed *RXTE* observations were detected to be in dip state, so an overall dip state spectrum was constructed for comparison. It was found that the spectral parameters are consistent with the models of diffuse emission (Valinia & Marshall 1998). Model estimated background was directly subtracted from each individual observation and the overall dip state spectrum was used as background in XSPEC. Systematic error of 2 per cent is applied during analysis to account for the uncertainties in the response matrix produced with PCARSP. 3–25 keV spectra of each individual non-dip observation were first modelled with power law with a high-energy cut-off and photoelectric absorption. Deviation of residuals around 20 keV confirmed the presence of cyclotron absorption feature reported by Mihara (1995), Cusumano

Table 2. Pulse period measurements of 4U 1907+09.

Epoch (MJD)	Pulse period (s)	Reference	Epoch (MJD)	Pulse period (s)	Reference
45576	437.483 ± 0.004	Makishima et al. 1984	53121.1	441.274 ± 0.005	Fritz et al. 2006
45850	437.649 ± 0.019	Cook & Page 1987	53133.4	441.297 ± 0.005	Fritz et al. 2006
48156.6	439.19 ± 0.02	Mihara 1995	53253.6	441.224 ± 0.010	Fritz et al. 2006
50134	440.341 ± 0.014	in't Zand et al. 1998	53291.3	441.201 ± 0.005	Fritz et al. 2006
50424.3	440.4854 ± 0.0109	Baykal et al. 2006	53314.0	441.188 ± 0.005	Fritz et al. 2006
50440.4	440.4877 ± 0.0085	Baykal et al. 2001	53324.7	441.183 ± 0.005	Fritz et al. 2006
50460.9	440.5116 ± 0.0075	Baykal et al. 2006	53443.4	441.154 ± 0.005	Fritz et al. 2006
50502.1	440.5518 ± 0.0053	Baykal et al. 2006	53473.3	441.139 ± 0.005	Fritz et al. 2006
50547.1	440.5681 ± 0.0064	Baykal et al. 2006	53503.8	441.124 ± 0.005	Fritz et al. 2006
50581.1	440.5794 ± 0.0097	Baykal et al. 2006	54281.5	441.1030 ± 0.0372	This work
50606.0	440.6003 ± 0.0115	Baykal et al. 2006	54291.0	441.1213 ± 0.0038	This work
50631.9	440.6189 ± 0.0089	Baykal et al. 2006	54315.0	441.1367 ± 0.0021	This work
50665.5	440.6323 ± 0.0069	Baykal et al. 2006	54338.2	441.1545 ± 0.0041	This work
50699.4	440.6460 ± 0.0087	Baykal et al. 2006	54353.3	441.1509 ± 0.0046	This work
50726.8	440.6595 ± 0.0105	Baykal et al. 2006	54367.3	441.1543 ± 0.0047	This work
50754.1	440.6785 ± 0.0088	Baykal et al. 2006	54381.3	441.1623 ± 0.0046	This work
50782.5	440.6910 ± 0.0097	Baykal et al. 2006	54396.2	441.1750 ± 0.0042	This work
51021.9	440.7045 ± 0.0032	Baykal et al. 2001	54410.9	441.1761 ± 0.0047	This work
51080.9	440.7598 ± 0.0010	Baykal et al. 2001	54426.0	441.1862 ± 0.0041	This work
51993.8	441.0484 ± 0.0072	Baykal et al. 2006	54442.1	441.1992 ± 0.0040	This work
52016.8	441.0583 ± 0.0071	Baykal et al. 2006	54456.1	441.2245 ± 0.0056	This work
52061.5	441.0595 ± 0.0063	Baykal et al. 2006	54470.4	441.2185 ± 0.0039	This work
52088.0	441.0650 ± 0.0063	Baykal et al. 2006	54486.3	441.2284 ± 0.0043	This work
52117.4	441.0821 ± 0.0062	Baykal et al. 2006	54509.4	441.2472 ± 0.0021	This work
52141.2	441.0853 ± 0.0082	Baykal et al. 2006	54532.3	441.2537 ± 0.0044	This work
52191.4	441.1067 ± 0.0046	Baykal et al. 2006	54546.8	441.2756 ± 0.0046	This work
52217.2	441.1072 ± 0.0077	Baykal et al. 2006	54561.6	441.2657 ± 0.0043	This work
52254.3	441.1259 ± 0.0074	Baykal et al. 2006	54584.3	441.2855 ± 0.0022	This work
52292.0	441.1468 ± 0.0065	Baykal et al. 2006	54607.1	441.3195 ± 0.0043	This work
52328.8	441.1353 ± 0.0090	Baykal et al. 2006	54629.6	441.3301 ± 0.0022	This work
52739.3	441.253 ± 0.005	Fritz et al. 2006	54652.1	441.3307 ± 0.0043	This work
52767.1	441.253 ± 0.005	Fritz et al. 2006	54667.2	441.3549 ± 0.0044	This work
53083.9	441.283 ± 0.005	Fritz et al. 2006	54682.1	441.3596 ± 0.0044	This work

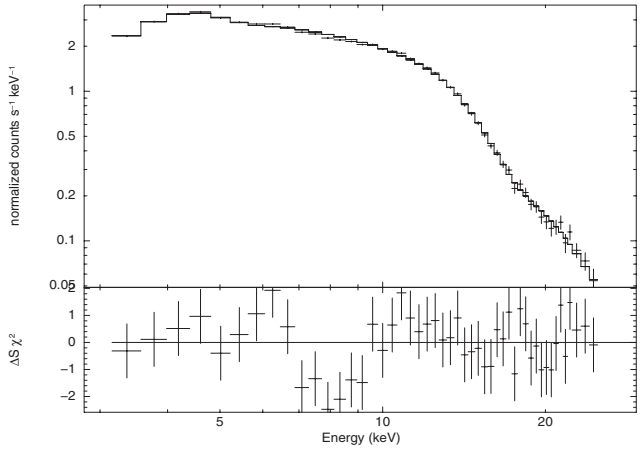

Figure 4. Average spectrum of all non-dip observations and the folded model is plotted. The bottom panel shows the residuals of the fit.

et al. (1998) and Makishima et al. (1999). Among the several models tested to fit the fundamental cyclotron line at ∼19 keV, best results were obtained by cyclotron absorption line model 'cyclabs' (Makishima et al. 1990). We first tried to fix the line energy to the reported value 18.9 keV, but better statistics is achieved when it is set free. The line energies were found to vary between ∼15.0 and ∼19.4 keV including 1σ errors, which are consistent with the previous studies.

The supernova remnant W49B has a strong emission feature at ∼6.4 keV (Miceli et al. 2006), but after a proper background subtraction, we did not find a significant iron line complex feature from 4U 1907+09. Although average spectrum (see Fig. 4) has deviating residuals around 7 keV which may correspond to iron line, adding a Gaussian component to the spectral model did not improve the fit.

In order to investigate orbital phase dependence of orbital variations of spectral parameters and X-ray flux, we present orbital phase resolved spectroscopy of the source in Fig. 5. Sample spectral parameters corresponding to different orbital phases are listed in Table 3.

5 CONCLUSION

After more than 15-yr long spin-down episode with an almost constant spin-down rate of $\dot{\nu} = -3.54(2) \times 10^{-14}$ Hz s^{-1} (Baykal et al. 2001), *RXTE* observations between 2001 March and 2002 March showed a ∼0.6 factor of decrease in spin-down rate compared to long-term spin-down rate of the source. From the observations of *INTEGRAL* between 2003 March and 2005 September, Fritz et al. (2006) found that source was spinning-up with a rate of 2.58×10^{-14} Hz s^{-1}. We found, in this work, that the source began to spin-down again with a spin-down rate of $-3.59(2) \times 10^{-14}$ Hz s^{-1} which is pretty close to the previous long-term spin-down rate of the source.

According to Ghosh & Lamb (1979) model, net torque exerted on the neutron star by the accreting matter from a prograde accretion disc can be expressed as

$$N = I\dot{\Omega} = n(\omega_s)\dot{M}l, \quad (2)$$

where I is the moment of inertia of the neutron star, $\dot{\Omega}$ is the spin frequency derivative, $n(\omega_s)$ is the dimensionless torque, $\dot{M}$ is mass accretion rate and l is specific angular momentum of the accreting matter. Here, ω_s is the fastness parameter defined as the ratio of

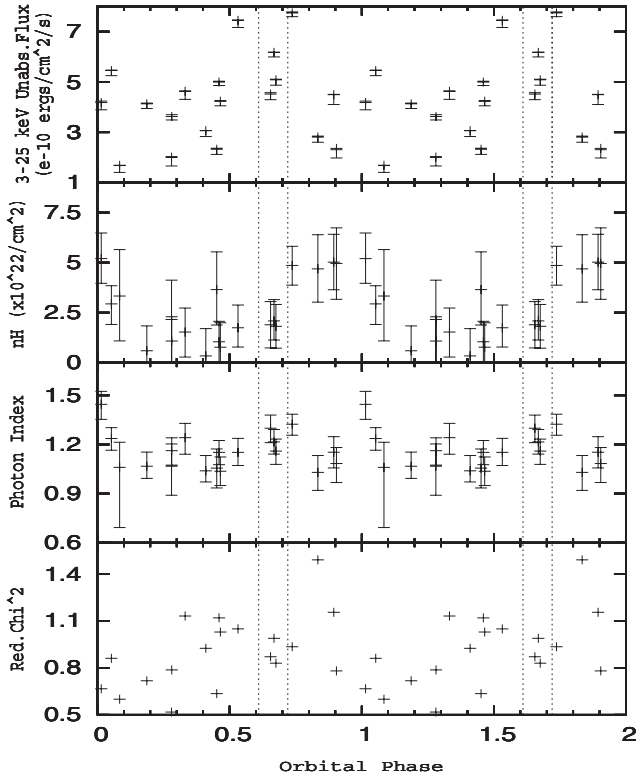

Figure 5. Orbital variations of the spectral parameters are plotted. Errors are calculated for 68 per cent confidence level. The dashed vertical lines indicate the time of periastron passage within 1σ.

neutron star's spin frequency to the Keplerian frequency at the magnetospheric radius, which is almost equal to the accretion disc's inner radius.

Dimensionless torque, $n(\omega_s)$ in equation (2), is the ratio of the total (magnetic and material torque) to the material torque. It is, for a slowly rotating neutron star ($\omega_s < 0.35$–0.95), expected to be positive and of the order of unity leading to spin-up of the star, whereas it is expected to be negative for a fast rotating neutron star ($\omega_s \gg 0.35$–0.95) leading to spin-down of the star (Ghosh & Lamb 1979; Wang 1995; Li & Wang 1996, 1999) . Since the dimensionless torque depends on the fastness parameter (and thus the magnetospheric radius), it decreases and may even be negative with an increase in magnetic field or decrease in mass accretion rate. Decrease in mass accretion rate leads to a decrease in X-ray flux and due to the accretion geometry changes, X-ray spectral variations may also be evident.

For 4U 1907+09, observed torque reversal cannot simply be explained by Ghosh & Lamb (1979) model since spin-up episode observed by *INTEGRAL* and spin-down episodes with different spin-down rates have not shown significant X-ray flux and X-ray spectral variations (Baykal et al. 2001, 2006; Fritz et al. 2006). Using this model, it is also difficult to explain similar spin rate magnitudes observed in spin-down and spin-up episodes of 4U 1907+09. Absolute value of the spin rate has always been found to be ~ 2–3×10^{-14} Hz s^{-1}.

In case of accretion via stellar wind, simulations showed that transition from spin-down to spin-up is possible even when there is not significant mass accretion rate change (Anzer, Börner & Monaghan 1987; Taam & Fryxell 1988a,b, 1989; Blondin et al. 1990; Murray, de Kool & Li 1999). However, torque reversal timescale of 4U 1907+09 is of the order of years which is much greater

Table 3. Sample spectral parameters of 4U 1907+09.

Observation ID	93036-01-29-00	93036-01-04-00	93036-01-16-00	93036-01-10-00
Observation mid-time (MJD)	54675	54300	54479	54389
Orbital phase	0.05	0.28	0.67	0.89
$n_{\rm H}$ (10^{22} cm^{-2})	$2.94^{+0.91}_{-1.03}$	$1.08^{+1.21}_{-1.08}$	$2.09^{+1.06}_{-0.96}$	$5.02^{+1.39}_{-1.38}$
Power-law photon index	$1.24^{+0.07}_{-0.07}$	$1.16^{+0.08}_{-0.09}$	$1.22^{+0.08}_{-0.07}$	$1.15^{+0.10}_{-0.10}$
Power-law normalization (10^{-2} counts cm^{-2} s^{-1})	$3.90^{+0.65}_{-0.59}$	$2.19^{+0.45}_{-0.39}$	$4.00^{+0.75}_{-0.60}$	$2.64^{+0.67}_{-0.53}$
Cut-off energy (keV)	$12.26^{+0.82}_{-0.35}$	$12.74^{+1.01}_{-0.44}$	$12.88^{+0.90}_{-0.74}$	$12.61^{+0.98}_{-0.74}$
E-folding energy (keV)	$7.67^{+1.54}_{-0.78}$	$7.27^{+1.96}_{-1.26}$	$10.88^{+2.49}_{-1.73}$	$8.78^{+3.89}_{-2.19}$
Cyclotron depth	$0.41^{+0.13}_{-0.19}$	$0.47^{+0.23}_{-0.24}$	$0.43^{+0.13}_{-0.13}$	$0.37^{+0.30}_{-0.13}$
Cyclotron energy (keV)	$16.74^{+0.65}_{-0.59}$	$16.70^{+0.78}_{-0.76}$	$16.63^{+0.58}_{-0.58}$	$17.17^{+1.23}_{-1.66}$
Cyclotron width (keV)	$1.00^{+1.91}_{-1.00}$	$1.14^{+1.47}_{-1.14}$	$1.95^{+0.98}_{-0.95}$	$2.53^{+1.79}_{-2.53}$
3–25 keV unabsorbed flux (10^{-10} erg cm^{-2} s^{-1})	$5.46^{+0.02}_{-0.21}$	$3.62^{+0.08}_{-0.14}$	$6.18^{+0.01}_{-0.18}$	$4.50^{+0.02}_{-0.22}$
Reduced χ^2 (41 dof)	0.86	0.79	0.99	1.16

than the typical time-scale of torque reversals in the simulations, found to be only of the order of hours. Moreover, 4U 1907+09 has shown transient quasi-periodic oscillations (QPOs) which is a sign of the presence of an accretion disc (in't Zand et al. 1998; Mukerjee et al. 2001; Baykal et al. 2006).

It may also be possible that negative torques (corresponding to spin-down episodes) may come from a retrograde Keplerian accretion disc (Nelson et al. 1997). Spin-down torques may also be the result of an advection dominated sub-Keplerian disc for which the fastness parameter should be higher than that of the rest of the Keplerian disc causing a net spin-down (Yi, Wheeler & Vishniac 1997) or the warping of the disc so that the inner disc is tilted by more than 90° (van Kerkwijk et al. 1998). Torque and X-ray luminosity correlation is expected from these models which is not found for 4U 1907+09.

A recent model of Perna, Bozzo & Stella (2006) explains torque changes in accreting neutron stars without a need for retrograde discs. In this model, the scenario in which the neutron star's magnetic field is tilted with respect to the axis of rotation of the neutron star is considered. For an accretion disc located in the neutron star's equatorial plane, the magnetic field strength depends on the azimuthal angle and thus the location of magnetospheric radius is variable. This can lead to regions in the disc where the propeller effect is locally at work, while accretion from other regions is possible. Perna et al. (2006) show that this accretion geometry may cause cyclic torque reversal episodes without a need for significant mass accretion rate variations.

4U 1907+09 has an eccentric orbit and shows occasional X-ray flux dips (in't Zand et al. 1997). These are indications of the transient accretion disc formation around the neutron star. On the other hand, model of Perna et al. (2006) is proposed for persistent prograde accretion discs like Ghosh & Lamb (1979) model. To understand torque reversal of 4U 1907+09, transient nature of the accretion should also be taken into account.

From Fig. 5, orbital dependence of $n_{\rm H}$ is evident, on the other hand, there is no significant variation of power-law index. $n_{\rm H}$ increases just after the periastron due to the accretion flow at the periastron passage and it remains at high values until the apastron. Roberts et al. (2001) also found similar $n_{\rm H}$ dependence on orbital phase and interpreted this $n_{\rm H}$ excess as the neutron star passing through an equatorially enhanced matter envelope in an inclined orbit.

ACKNOWLEDGMENTS

SÇİ and AB acknowledge support from TÜBİTAK, the Scientific and Technological Research Council of Turkey through project 106T040 and EU FP6 Transfer of Knowledge Project "Astrophysics of Neutron Stars" (MTKD-CT-2006-042722). We thank Elif Beklen for useful discussions.

REFERENCES

Anzer U., Börner G., Monaghan J., 1987, A&A, 176, 235
Baykal A., Ínam G., Alpar M. A., In't Zand J., Strohmayer T., 2001, MNRAS, 327, 1269
Baykal A., İnam S. Ç., Beklen E., 2006, MNRAS, 369, 1760
Blondin J. M., Kallman T. R., Fryxell B. A., Taam R. E., 1990, ApJ, 356, 591
Chitnis V. R., Rao A. R., Agrawal P. C., Manchanda R. K., 1993, A&A, 268, 609
Coburn W., Heindl W. A., Rothschild R. E., Gruber D. E., Kreykenbohm I., Wilms J., Kretschmar P., Staubert R., 2002, ApJ, 580, 394
Cook M. C., Page C. G., 1987, MNRAS, 225, 381
Cox N. L. J., Kaper L., Mokiem M. R., 2005, A&A, 436, 661
Cusumano G., di Salvo T., Buderi L., Orlandini M., Piraino S., Robba N., Santangelo A., 1998, A&A, 338, L79
Deeter J. E., Boynton P. E., 1985, in Hayakawa S., Nagase F., eds, Proc. Inuyama Workshop, Timing Studies of X-Ray Sources. Nagoya Univ., Nagoya, p. 29
Fritz S., Kreykenbohm I., Wilms J., Staubert R., Bayazit F., Pottschmidt K., Rodriguez J., 2006, A&A, 458, 885
Ghosh P., Lamb F. K., 1979, ApJ, 234, 296
Giacconi R., Kellogg E., Gorenstein P., Gursky H., Tananbaum H., 1971, ApJ, 165, L27
in't Zand J. J. M., Strohmayer T. E., Baykal A., 1997, ApJ, 479, L47
in't Zand J. J. M., Baykal A., Strohmayer T. E., 1998, ApJ, 496, 386
Iye M., 1986, PASJ, 38, 463
Jahoda K., Swank J. H., Giles A. E., Stark M. J., Strohmayer T., Zhang W., Morgan E. H., 1996, Proc. SPIE, 2808, 59
Leahy D. A., Darbro W., Elsner R. F., Weisskopf M. C., Sutherland P. G., Kahn S., Grindlay J. E., 1983, ApJ, 266, 160
Li X.-D., Wang Z.-R., 1996, A&A, 307, L5
Li X.-D., Wang Z.-R., 1999, ApJ, 513, L845
Makishima K., Kawai N., Koyama K., Shibazaki N., 1984, PASJ, 36, 679
Makishima K. et al., 1990, PASJ, 42, 295
Makishima K., Mihara T., Nagase F., Tanaka Y., 1999, ApJ, 525, 978

Marshall N., Ricketts M. J., 1980, MNRAS, 193, 7P
Miceli M., Decourchelle A., Ballet J., Bocchino F., Hughes J. P., Hwang U., Petre R., 2006, A&A, 453, 567
Mihara T., 1995, PhD thesis, RIKEN, Tokyo
Mukerjee K., Agrawal P. C., Paul B., Rao R., Yadav J. S., Seetha S., Kasturirangan K., 2001, ApJ, 548, 368
Murray J. R., de Kool M., Li J., 1999, ApJ, 515, 738
Nelson R. W. et al., 1997, ApJ, 488, L117
Perna R., Bozzo E., Stella L., 2006, ApJ, 639, 363
Roberts M. S. E. et al., 2001, ApJ, 555, 967
Schwartz D. A., Griffiths R. E., Bowyer S., Thorstensen J. R., Charles P. A., 1980, AJ, 85, 549
Taam R. E., Fryxell B. A., 1988a, ApJ, 327, L73
Taam R. E., Fryxell B. A., 1988b, ApJ, 335, 862
Taam R. E., Fryxell B. A., 1989, ApJ, 339, 297
Valinia A., Marshall F. E., 1998, ApJ, 505, 134
van Kerkwijk M. H., van Oijen J. G. J., van den Heuvel E. P. J., 1989, A&A, 209, 173
van Kerkwijk M. H., Chakrabarty D., Pringle J. E., Wijers R. A. M. J., 1998, ApJ, 499, L27
Wang Y.-M., 1995, ApJ, 449, L153
Yi I., Wheeler J. C., Vishniac E. T., 1997, ApJ, 481, L51

This paper has been typeset from a TEX/LATEX file prepared by the author.